Characteristic Investigations of a New Three-Phase Flux-Switching Permanent Magnet Machine by FEM Simulations and Experimental Verification

Anyuan Chen, Njål Rotevatn, Robert Nilssen and Arne Nysveen
Department of Electrical Power Engineering
Norwegian University of Science and Technology, Trondheim, Norway

***Abstract* — In this paper a new flux-switching permanent magnet (FSPM) machine with 12 stator poles and 14 rotor poles is investigated, and compared to a machine with the same stator but 10 rotor poles. Two prototypes are studied by both finite element method (FEM) analysis and experimental measurements. The results show that the 12/14 pole prototype can provide about 7-12% higher torque, the torque ripple reduces from 8.5% to 5.1% and its synchronous inductance is also 15% higher. After optimization, the FEM simulation results show the 12/14 pole machine could provide 19% higher torque than the 12/10 pole machine and the torque ripple is further reduced to 2.3%.**

***Index Terms*--Flux-switching PM machine, FEM analysis, optimization, experimental measurements.**

I. Introduction

Flux-switching permanent magnet (FSPM) machines have PMs on the stator combined with doubly salient stator and rotor structure. They integrate the advantage of a conventional PM machine and a switched reluctance machine of having both high torque density and high reliability and are therefore preferable for the applications with harsh conditions. This type of machine has been presented in several papers [1]-[9], particularly the FSPM machine with 12 stator poles and 10 rotor poles, which has an essentially symmetrical and sinusoidal three-phase back EMF as well as relatively small torque ripple [2][4][6]. The detailed machine construction and operation principle have been presented in [7]-[9]. Here a new FSPM machine with 12 stator poles and 14 rotor poles mentioned in [3] is studied and compared to a 12/10 pole one. Their back EMF, electromagnetic torque and torque ripple are investigated by FEM analysis for two initially designed machines, of which all the values of stator tooth width, magnet thickness, slot opening, rotor tooth width and stator iron back thickness are the same and equal to one fourth of the stator pole pitch τ_s. To verify the results, an optimized 12/10 pole machine prototype presented in [11] and a newly built 12/14 pole machine prototype are tested. The experimental results are compared with the FEM results. At last, the 12/14 pole machine is optimized by FEM analysis to improve its output torque.

The work is supported by NFR.

II. Machine Construction

Fig. 1 shows the two initially designed FSPM machines with an outer diameter of 100 mm and an inner diameter of 50 mm. Both machines have exactly the same physical construction and winding arrangement except their rotor pole numbers. It should be noted that the positions of phase *b* and *c* in the 14-pole machine have interchanged compared to those in the 10-pole machine as can be seen from Fig. 1. In the FSPM machines each phase consists of four coils and each coil is concentrated around two stator teeth with a magnet inset in between as shown in Fig. 2, where only coil A1 and the stator teeth, magnets and rotor teeth around it are presented. At this position the resultant flux coupling each coil of phase *a* is zero. Due to the symmetrical constructions of these two machines, for each phase the flux in the corresponding coils 1 and 2 are respectively the same as in coils 3 and 4.

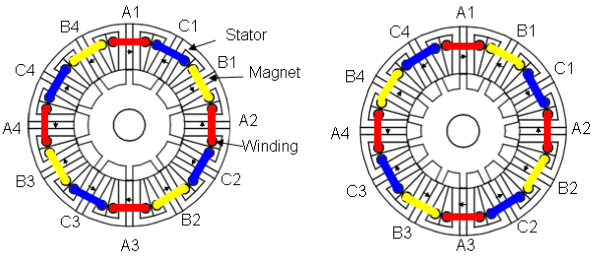

Fig. 1. (a) 12/10 pole (b) 12/14 pole machines.

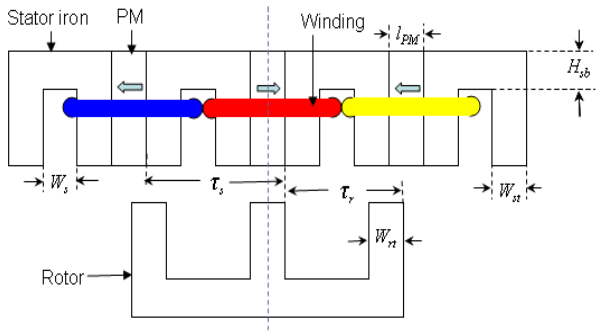

Fig. 2 Coil A1 at the zero flux position

III. FEM ANALYSIS AND COMPARISON

The flux variation in the coils with respect to the rotor position has been investigated by FEM simulations and shown in Fig. 3, where the flux in coil A1, A2 and their sum flux in one period of τ_r of the 12/14 pole machine have been presented. It is can be seen that the sum of the flux in A1 and A2 is essentially sinusoidal, and can be expressed as

$$\Phi_{A1}(t)+\Phi_{A2}(t)=\Phi_{\max}\cos(p_r\omega_m t) \quad (1)$$

where Φ_{max} is the peak value of the sum flux in coil A1, Φ_{A1}, and A2, Φ_{A2}, ω_m is the mechanical angular speed, P_r is the number of the rotor pole.

The induced phase EMF can be evaluated by

$$e(t)=-\frac{n_s}{2}\frac{d(\Phi_{\max}\cos(p_r\omega_m t))}{dt} \quad (2)$$

where n_s is the number of turn in one phase.

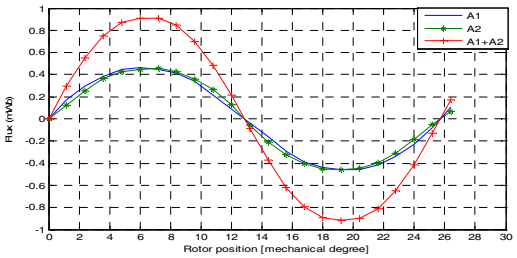

Fig. 3 Flux in coil A1, A2 and A1+A2

As can be seen from Fig. 3 by moving the rotor a displacement of $\tau_r/4$ from the zero flux position shown in Fig. 1 and Fig. 2, the total flux in A1 and A2 reaches its maximum value Φ_{max}. It is also observed that at this position the fluxes in coil A1 and A2 are the same, $\Phi_{A1(max)} = \Phi_{A2(max)}$, since the corresponding rotor tooth positions with respect to the coils A1 and A2 are the same, but at the opposite side of their corresponding magnets whose magnetization directions are also opposite as shown in Fig. 4. Fig. 5 depicts the flux distribution in coil A1 in a plain form. At this position the effective flux $\Phi_{A1(max)}$ coupling coils A1 for producing torque can be evaluated by (3).

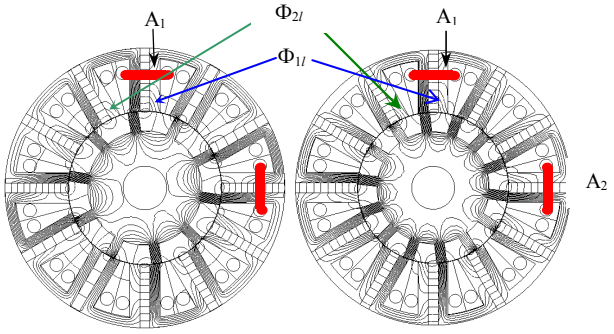

Fig. 4 Flux distribution at the maximum flux position of coil A (a) 12/10 pole machine (b) 12/14pole machine.

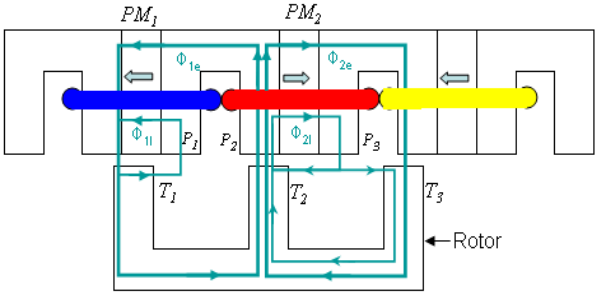

Fig. 5 Flux distribution in winding A1 when the total flux of A1 and A2 is maximum shown in Fig. 4.

$$\Phi_{A1(\max)}=\Phi_{1e}+\Phi_{2e} \quad (3)$$

where Φ_{1e} and Φ_{2e} are respectively the effective flux produced by magnets PM_1 and PM_2 (see Fig. 5) to contribute the torque production.

Eq. (3) can be re-written as

$$\Phi_{A1(\max)}=k_\sigma W_{st} L B_t \quad (4)$$

where W_{st} is the stator tooth width, L is the machine active axial length, B_t is the flux density in the top of stator tooth P_2, k_σ is the leakage factor to represent the leakage flux Φ_{2l} back to the rotor via P_3 at the maximum flux position. k_σ is always less than unity.

Assuming that all the coils of each phase are connected in series, substituting (1), (3) and (4) into (2) yields

$$e(t)=k_\sigma n_s p_r \omega_m W_{st} L B_t \sin(p_r\omega_m t) \quad (5)$$

The torque expression of the FSPM machine is derived as follows:

Assuming the induced phase voltage is in phase of the phase current, the electromagnetic torque produced by an electrical machine can be calculated by

$$T=\eta m E_{ph} I_{ph}/\omega_m . \quad (6)$$

where m is the phase number, η is the machine efficiency, E_{ph} is the *rms* value of the induced phase voltage and can be expressed as (7) from (5). I_{ph} is the *rms* value of the phase current and determined by (8).

$$E_{ph}=k_\sigma n_s p_r \omega_m W_{st} L B_t/\sqrt{2} \quad (7)$$

$$I_{ph}=\pi D_o \lambda S/2mn_s \quad (8)$$

where λ is the ratio of the machine inner- and outer-stator diameters, D_o is the machine outer-stator diameter, S is the electrical loading.

Substituting (7) and (8) into (6) yields

$$T=\frac{\sqrt{2}\pi}{4}k_\sigma P_r \lambda D_o S W_{st} L B_t \eta \quad (9)$$

It is clearly shown from (7) and (9) that the machine back EMF and output torque are proportional to P_r. In case of keeping other parameters in (9) unchanged, the 12/14 pole machine would provide 40% higher back EMF and torque than the 12/10 pole machine, but actually the values of k_σ and B_t of the 12/14 pole machine will decrease due to the shorter rotor pole pitch leading to the increased flux leakage Φ_{1l} and Φ_{2l} between the stator and rotor as shown in Fig. 4, where the total flux coupling all the coils of phase *a* is maximum. So the increments of the torque and back EMF of the 12/14 pole machine will be less than 40% as shown in Fig. 6 and Fig. 7, where the back EMFs and the output torques from FEM analysis have respectively been presented for the two machines shown in Fig. 1. Both machines provide sinusoidal and symmetrical back EMFs for three phases. The back EMFs and output toque of the 12/14 pole machine are about 30% higher and its torque ripple is much less compared to the 12/10 pole machine.

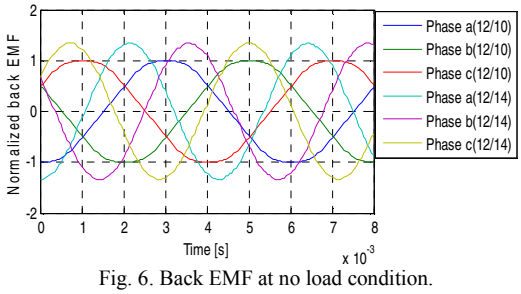

Fig. 6. Back EMF at no load condition.

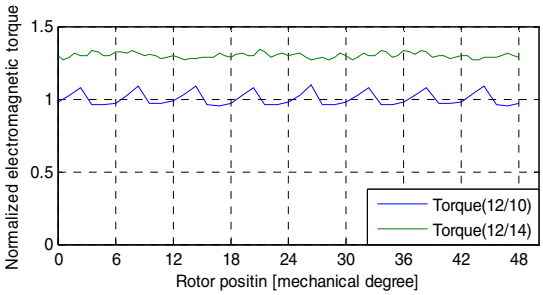

Fig. 7. Output torque.

IV. Prototype Machines

To verify the results, a 12/10 pole machine prototype presented in [11] is employed. The 12/10 pole machine has been optimized according to the research presented in [1] and [4] to improve its output torque by increasing the rotor width 46% of the original one and reducing the stator back-iron thickness to 70% of the stator tooth width. Table 1 lists the machine parameters. It should be noted the stator tooth width was chosen to be slightly wider than the magnet thickness to decrease the iron saturation in the stator teeth. In order to easily assemble the machine, a stator iron bridge with the thickness of 1.5mm was added between each U-shape stator core as shown in Fig. 8. The FEM simulations show the bridges just slightly decreases the machine output torque, 1.1%, caused by the leakage flux through the highly saturated iron bridges.

A 12/14 pole machine prototype is built in the laboratory based on the 12/10 pole machine by simply replacing a 14 pole rotor instead of the 10 pole one, keeping the rotor tooth width unchanged.

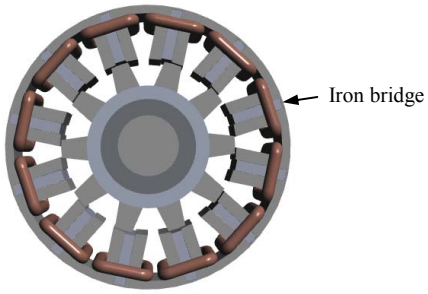

Fig. 8 3D view of the 12/10 pole prototype.

Table 1 PROTOTYPE PARAMETERS

Phase number	3
Number of stator pole	12
Number of rotor pole	10 and 14
Outer stator diameter	210 mm
Inner stator diameter	130 mm
Airgap length	1 mm
Active axial length	50mm
Number of turns per pole	174
Magnet remanence	1.16T
Magnet relative permeability	1.05
Rated phase current (rms)	3.4A
Rated speed	400rpm
Rotor tooth width top/bottom	13/18 mm
Stator back iron width	6.3mm
Stator tooth width	8.9mm
Magnet width	8mm
Rotor tooth height	18.3mm
Stator iron bridge	1.5mm

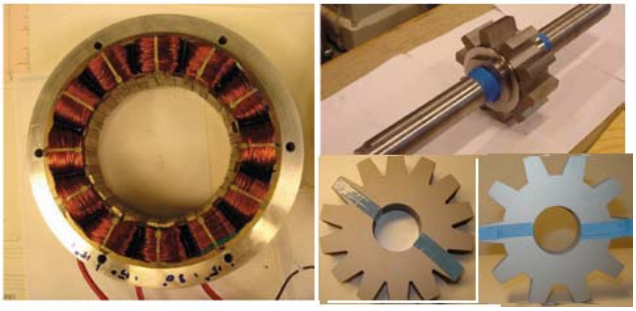
(a) (b)
Fig. 9 Machine prototype (a) stator (b) rotors.

V. Simulations and Measurements

Fig. 9 shows the machine prototypes in the laboratory. The characteristics of these two prototypes are firstly investigated by 2D FEM simulations and then compared with experimental measurements. For the discussed machines having a relatively small axial length, the influence of end effect that is not included in the 2D FFM simulations is significant and can decrease the flux linkage, the phase back EMF and the output torque by ~10% according to the research presented in [1]. In order to take the end effect into account, afterwards all the values of the back-EMF and the output torque from 2D

FEM simulations presented in this paper have been corrected by multiplying 0.9.

Fig. 10 and Fig. 11 respectively show the induced back EMFs at no-load condition by the FEM calculations and experimental measurements for the 12/10 pole and 12/14 pole machines. As can be seen that both machines have essentially sinusoidal back EMF waveforms and they are symmetrical for three phases. Their total harmonic distortions (THD) are investigated by Fourier analysis and are respectively less than 1.5% and 1.2%. It is also observed that the induced back EMF of the 12/14 pole machine is only ~10% higher than that of the 12/10 pole machine. The reason is that the performance of the 12/10 pole machine can be improved with relatively high saturation in the stator teeth and the increased rotor teeth width, but not for the 12/14 pole machine because of its rotor pole pitch less than its stator pole pitch leading to a large amount of leakage flux coming back from the neighbor teeth as shown in Fig. 17. This is proven later by FEM simulations in the section of *optimization of 12/14 pole machine.*

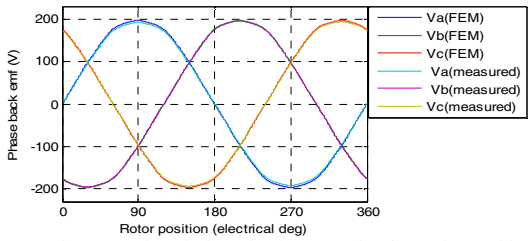

Fig. 10 Induced phase back EMF of 12/10 pole machine.

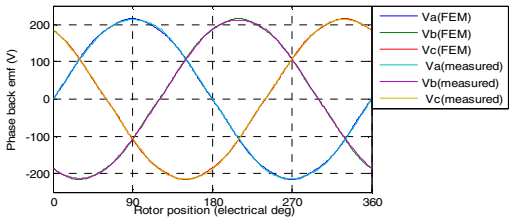

Fig. 11 Induced phase back EMF of 12/14 pole machine.

Fig. 12 presents the output torques of both machines at the rated current of 3.4A by FEM calculations. Their average torques are shown in Fig. 13 and compared with the measured values. The results show that the average torque of the 12/14 pole machine is 7~12% higher than that of the 12/10 pole machine. The peak to peak torque ripple in percentage of the 12/14 pole machine, 5.1%, is also less than that of 12/10 pole machine, 8.5%, as can be observed from Fig. 12.

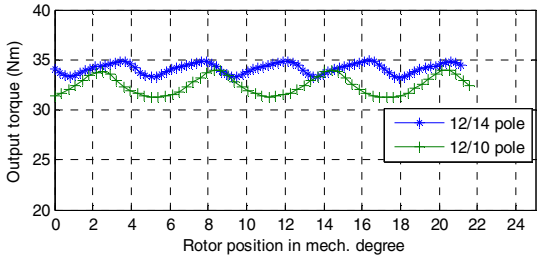

Fig. 12 Output torque from FEM calculations.

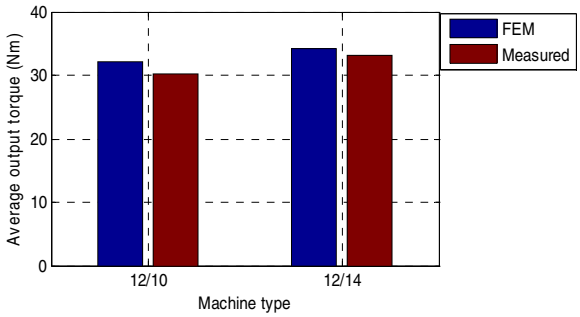

Fig. 13 Average output torque at the rated current.

Fig. 14 depicts the cogging torque of these two machines by FEM calculations. And the result shows that the peak cogging torques are respectively 1.2 Nm and 1.1 Nm for the 12/10 and 12/14 pole machines, but the measured peak cogging torque is about 1.6 Nm for both machines. The reason is because the stator has become elliptic during the machine assembly, and the airgap in vertical direction of the machine cross-section become ~0.8mm, whilst in horizontal direction it is ~1.2 mm. Fortunately, due to the high saturation in the stator teeth, the uneven airgap does not significantly influence the flux distribution in the airgap, so the measured back EMFs of three phases are almost the same shown in Fig. 10 and Fig. 11, the differences of their peak values are less than 1.5%.

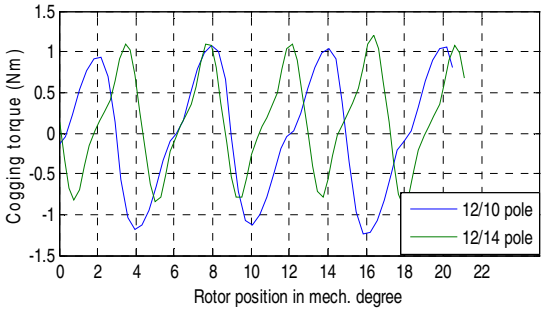

Fig. 14 Cogging torque of 12/10 and 12/14 pole FSPM machine.

Fig. 15 and Fig. 16 respectively present *d*- and *q*-axis inductances of the two machines from both the FEM simulations and measurements. Due to the larger iron area along the rotor circumference determined by the product of the rotor number and rotor tooth width, the measured inductance of the 12/14 pole machine is about 15% higher than that of the 12/10 pole machine.

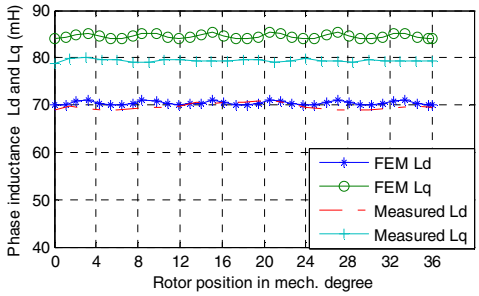

Fig. 15 Phase inductance of 12/10 pole machine.

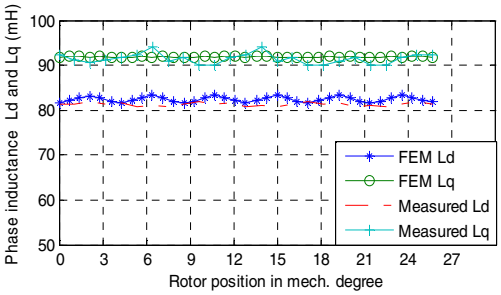

Fig. 16 Phase inductance of 12/14 pole machine.

Both machine efficiencies are also measured at the rated speed and the rated current, and they are almost the same of 84%. The 12/14 pole machine does not have a higher efficiency as expected even it provides higher torque with the same copper loss. This is because its iron loss approximated from (10) [10] have increased more than 40% due to the 40% higher electrical frequency and the increased iron volume in the rotor, whilst its torque increment is only ~10%.

$$P_{Fe} = 0.078Wf(100+f)B_{Fe}^2 G_{Fe} 10^{-3} \qquad (10)$$

where W is the specific loss factor in W/kg, G_{Fe} is the weight of the iron part, while B_{Fe} is the peak flux density in the corresponding iron part, f is the electrical frequency.

VI. Optimization of 12/14 Pole Machine

The performance of the 12/14 pole machine can be improved by optimization. As can be seen from Fig. 17, at the maximum resultant flux position of each phase (here phase *a*) the flux leakage is high due to the high flux saturation, 2.1T, in the stator tooth top and the relatively small space between the adjacent rotor teeth.

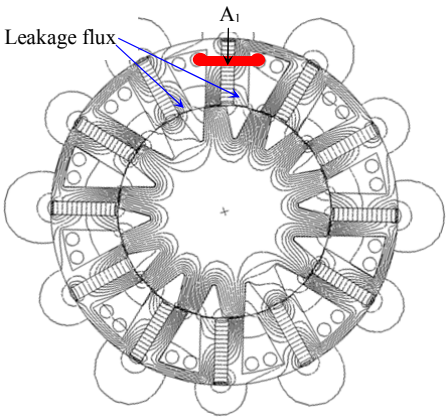

Fig. 17 Flux distribution in the 12/14 pole prototype machine at the maximum resultant flux position of coil A.

The flux saturation can be reduced by decreasing the magnet thickness. On the other hand, the total magnetic flux produced by the magnets also decreases along with a reduction of the magnet thickness. So there is an optimal magnet thickness providing the highest torque. Fig. 18 shows the output torques with respect to different magnet thicknesses. Their average torques and peak to peak torque ripples have also been presented in Fig. 19. It is shown that with 7mm magnet thickness the machine provides the highest average output torque of 35.3 Nm, whilst with 6mm magnet thickness the machine has the lowest torque ripple of 2.4%. It should be noted that during the optimization procedure, the stator slots, phase winding and phase current are kept unchanged, so the copper loss is the same as before the optimizations.

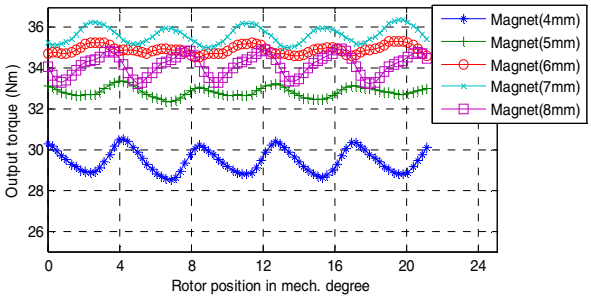

Fig. 18 Output torque with different magnet widths

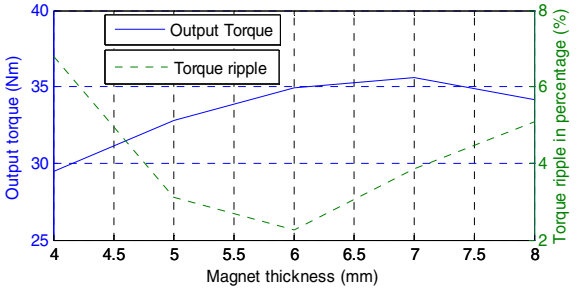

Fig. 19 Average torque and torque ripple (peak to peak).

By reducing the rotor tooth width to increase the space between the adjacent rotor teeth can further reduce the flux leakage. Meanwhile the flux saturation in the rotor teeth will also increase along with a decrease of the rotor tooth width. So there is an optimal rotor width providing the highest torque. The output torques with varied rotor tooth widths are illustrated in Fig. 20 while the magnet thickness is fixed to 7mm. Their average torques and torque ripples are provided in Fig. 21. It is observed that with 11mm rotor tooth width the machine has both a high output torque of 38.3 Nm and a small torque ripple of 2.3%. Compared to the 10/12 pole machine, the output torque is ~19% higher and the torque ripple is also further reduced.

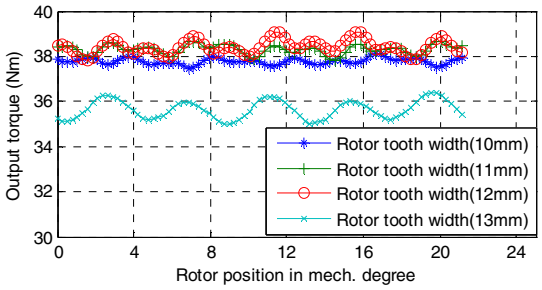

Fig. 20 Output torque with different rotor widths (fixed 7mm magnet).

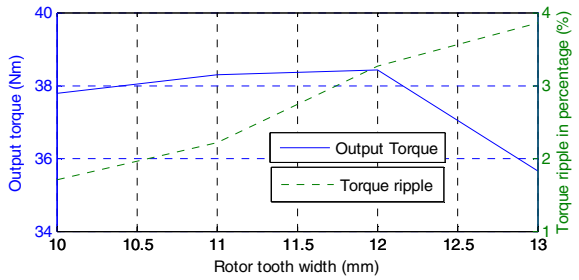

Fig. 21 Average torque and torque ripple in Fig. 20.

VII. CONCLUSION

In this paper a new 12/14 pole FSPM machine has been investigated by both FEM analysis and experimental measurements. Compared to the 12/10 pole machine, the results show that the 12/14 pole machine has the following characteristics:

- The 12/14 pole machine also has a symmetrically sinusoidal three-phase back EMF as shown in Fig. 6 and Fig. 11, and the frequency is 40% higher.
- With the same copper loss, the 12/14 pole machine can provide higher output torque. The FEM simulations and the experimental measurements show the original 12/14 pole machine prototype can provide 7~12% higher torque compared to the optimized 12/10 pole one, and the FEM simulations show the optimized 12/14 pole machine could provide ~19% higher torque.
- Less toque ripple is achieved. The FEM simulation results show that the 12/14 pole prototype has decreased the torque ripple to 5.1%, whilst 8.5% for the 12/10 pole one. The torque ripple can be further reduced to 2.3% after optimization.
- Better filed-weakening capability because of the higher synchronous inductance. Due to the larger iron area along the rotor circumference, the 12/14 pole machine has higher inductance. This is proved by both FEM simulations and the measurements of the prototypes.
- Higher efficiency is expected for low speed applications where the copper loss is the dominant loss in machines.

References

[1] Z. Q. Zhu, Y. Pang, D. Howe, S. Iwasaki, R. Deodhar, and A. Pride, "Analysis of electromagnetic performance of flux-switching permanent magnet machines by non-linear adaptive lumped parameter magnetic circuit model," IEEE Transactions on Magnetics, Vol.41, No.11, pp.4277-4287, November 2005.

[2] Zhang, Z. Chen and M. Cheng, "Design and comparison of a novel stator interior permanent magnet generator for direct-drive wind turbines", IET Renewable Power Generation, December, 2007, Vol.1 pp 203-210.

[3] J. T. Chen, Z. Q. Zhu, A. S. Thomas and D. Howe, "Optimal combination of stator and rotor pole numbers in flux-Switching PM brushless AC machines", the proceeding of ICEMS 2008, Vol. 44 pp 4659 – 4667.

[4] Z.Q. Zhu, Y. Pang, J. T. Chen, Z. P. Xia, D. Howe, "Influence of design parameters on output torque of flux-switch permanent magnet machines", IEEE Vehicle Power and Propulsion Conference (VPPC), September 3-5, 2008, Harbin, China.

[5] W. Z. Fei and J. X. Shen, "Comparative study and optimal design of PM switching flux motors". UPEC'06, 6-8 Sept. 2006, Vol.2 pp 695-699.

[6] Emmanuel Hoang, Michel Lecrivain, Mohamed Gabsi, "A new structure of a switching flux synchronous polyphased machine with hybrid excitation", the proceeding of Power electronics and applications, 2007 European conference, pp 1-8.

[7] Wei Hua, Ming Cheng, Z. Q. Zhu and D. Howe, "Design of flux-switching permanent magnet machine considering the limitation of inverter and flux –weakening capability". IEEE 2006, pp 2403-2410.

[8] Jiangzhong Zhang, Ming Cheng and Zhe Chen, "Optimal design of stator interior permanent magnet machine with minimized cogging torque for wind power application", Energy Conversion and management 49, 2008, pp 2100-2105.

[9] Wei Hua, Ming Cheng, Z. Q. Zhu and David Howe, "Analysis and optimization of back EMF waveform of a flux-switching permanent magnet motor", IEEE Transactions on Energy Conversion, VOL. 23, NO. 3, September 2008, pp 727-733.

[10] Chandur Sadarangani, "Electrical machines", ISBN 91-7170-627-5, KTH Högskoletryckeriet, Stockholm, Sweden.

[11] Njål Rotevatn, "Design and testing of flux switched permanent magnet machines", Master thesis, Jul. 2009, Norwegian University of Science and Technology, Trondheim, Norway.